INTERNATIONAL JOURNAL OF AUTOMOTIVE AND MECHANICAL ENGINEERING (IJAME)
ISSN: 2229-8649 e-ISSN: 2180-1606
VOL. 20, ISSUE 1, 2023, 10175 – 10191
DOI: https://doi.org/10.15282/ijame.20.1.2023.03.0788

ORIGINAL ARTICLE

Experimental Study and Predictive Modelling of Fused Deposition Modelling (FDM) Using TOPSIS and Fuzzy Logic Expert System

S. Prabhu[1], M. Uma[2], J. Jaishwin[1] and M. Nikhil[1]

[1]Department of Mechanical Engineering, SRM Institute of Science and Technology, Kattankulathur, Chennai 603203, India
[2]Department of Computational Intelligence, SRM Institute of Science and Technology, Kattankulathur, Chennai 603203, India

ABSTRACT – Fused deposition modeling (FDM) is a well-liked additive fabrication method used to manufacture prototypes and components in industries. The quality of the 3D printed component depends on the temperature profile between the layers of the printed components and the process parameters. The deviations in the quality of manufactured components can be established using tools of metrology, including Coordinate-Measuring Machine and Machine Vision. This research is to determine the effect of temperature on the aforementioned phenomenon by using collected data to build a predictive model. The leading factor effect intrigue is stressed for the correlative closeness coefficient (Cn*) and Technique for Order of Preference by Similarity to Ideal Solution(TOPSIS). The most favorable combinations of the experiment were obtained from the response diagram at a layer thickness of 0.3 mm, print speed of 80 mm/sec, and infill percentage of 20%. It is noted that the parameters have a contribution of 55.60%, 33.16%, and 0.15%, respectively. The majority of agreeable combinations of the investigations were acquired from the main factor effect response diagram, a layer thickness of 0.3 mm, printing FDM speed of 80 mm/sec, and an infill percentage of material is 20% for maximizing the temperature gradient and minimizing shrinkage and warpage. A fuzzy logic expert system was used to predict the shrinkage allowances precisely with less than 5% error.

ARTICLE HISTORY
Received: 7th Sept2022
Revised: 21st Dec 2022
Accepted: 4th Jan 2023
Published: 30th Mar 2023

KEYWORDS
Fused deposition modeling;
TOPSIS;
ANOVA;
Fuzzy logic analysis;
Regression analysis

INTRODUCTION

As product complexity increases, there is a need for intelligent and novel manufacturing techniques. There is a necessity to devise an effective, optimal and universally usable additive manufacturing technique by reducing the build time, improving quality, and lowering deployment costs. Fused deposition modeling (FDM) is not yet researched deeply enough to deploy in all real-world applications. There are several challenges and drawbacks, such as limited part size due to fixed bed size, void formation in between the layers, and shrinkage and warpage defects can be observed. FDM cannot be used to build structural components due to the uneven layer adhesion, which results in an anisotropic nature and irregular mechanical properties. Sood et al. [1] concluded that FDM is thermally driven by undertaking/conducting a parametric appraisal of the process. In the FDM process, three-dimensional parts are created from polymer-based filament by melting and depositing in layers that fuse together. The material is subjected to cooling and heating cycles resulting in non-uniform temperature gradients. The authors reported that shrinkage occurred due to the cooling of the component as a result of the thermal gradient between the surrounding air and the melting temperature at which the material was extruded. When cooled, the deposited thermoplastic fiber was subjected to contraction. Shrinkage was attributed to the development of internal stress as a result of the contraction of the deposited fibers. The deposited material was likely to get deformed and might not match the designed dimension due to the presence of non-uniform stresses. The main motive of their study was to abate and reduce the change in the percentage of width, diameter, length, and thickness of the material. Antonio Armillotta et al. [2] aimed to characterize the warpage defect on components manufactured from resin blocks using an automatic breaking system with relation to the geometric dimension in the thickness of deposited layers. Their study highlighted that warpage is a structural defect that is usually seen in thin, flat components. The filament is extruded at melting temperature, which reduces further due to the high thermal gradient to circumferential air. This leads to a phenomenon causing shrinkage and leads to compressive and tensile stresses all over the segment. Further, it is dependent on process criterion, component geometry and material properties. It was concluded by the authors that part geometry had a sizable impact on the warpage. It increased linearly with length, was directly proportional to layer thickness and decreased with increasing height of the part pointing to the instance of highest contortion.

Dario Croccolo et al. [3] conducted experiments with a raster angle set between +45/45 degrees. Printed beads were inclined similarly to the axis and loading direction of the specimen. The air gap value was chosen to be zero millimeters, while layer thickness was fixed at 0.25 mm. The study considered the FDM of slender beam components. The length was higher than the width and height. The total load was shared in each of these elements between inclined and longitudinal rasters resulting in beads that could sustain the load of the previously deposited layers. Hardikkumar Prajapati et al. [4] studied the dispensing of filament over glass. They found that the transition temperature was an important factor to be

*CORRESPONDING AUTHOR | S.Prabhu | ✉ prabhus@srmist.edu.in

considered in additive manufacturing. By using infrared thermography, the measurement distributions in the filament standoff region were noted. It was found that parameters like mass flow rate, the diameter of the filament, cooling conditions, and heat capacity had a considerable influence. Heat transfer occurred in the filament bed, and the authors/study concluded that the nature of the bed determined the overall quality of the 3D-printed part.

Ehsan Malekipour et al. [5] explained that warpage defect is directly related to the thermal characteristics as well as the temperature distribution of deposited layers. Warpage occurs mainly due to the thermal interaction between previously deposited and current layers. The thermal gradient between the new layer, which is at a higher temperature compared to the existing layer, causes the top layer to contract relative to the preceding one as a result of induced thermal stresses. This contraction causes warpage. The experimental parameters used to print the specimens were a honeycomb fill pattern and 30% infill density. Improvement was observed in certain mechanical properties as the mean temperature of printed layers was increased. However, this led to a poor surface finish and possible quality defects. The plotted temperature data collected throughout the printing process across layers pointed to a lower uniformity in temperature changes between the first layers closer to the build platform, which was also heated. Furthermore, it was noticed that the temperature was evenly distributed as the building of layers progressed from midway to the topmost layer of the part. The influence of the temperature changes across layers on the final quality of the printed part was confirmed by the study of the temporal plot.

Morales et al. [6] conducted an experimental study by printing five samples of each specimen with five distinct interlayer wait durations: 20, 15, 10, 5 and 0 to investigate the effects of layer adhesion and inter-layer cooling effects on shear and compressive abilities of filament material of Acrylonitrile Butadiene Styrene (ABS) in FDM. They reported that the plastic material was thermally strong if the preceding layer had cooled completely. Poorly adhered layers resulted in decreased strength. Augmented wait times led to reduced quality of the shear section formed. It was concluded that since all parts were produced using parameters influencing printing which were identical apart from interlayer waiting duration, the errors were a result of wait durations in-between printing subsequent layers of comparable features. Therefore, printing processes like finer 3D geometries and bigger parts would naturally lead to deterioration in the quality of the printed structure due to the poor adhesion of layers, which was a result of the longer interlayer wait time that was required for these parts. Mohamed [7] discussed FDM process parameters which were optimized using different design of experiment techniques. The optimization was used to examine the FDM parameters and also to analyze the future trends of FDM.

Raykar et al. [8] reported that FDM was a process that is used for additive manufacturing of plastic components along with other processes. They found that the FDM process was governed by several other process parameters that had an impact on print performance. Using the VIKOR decision-making technique, the optimal process parameters were determined. Coogan et al.[9] conducted experiments to study the processing melt temperatures using thermocouple and custom pressure transducers. Various parameters were considered for rheological corrections. The study observed that the designed inline FDM rheometer (FDM Rheo) provided very accurate measurements. Tlegenov et al. [10] studied nozzle clogging and its monitoring techniques. They found that there were only a limited number of techniques available to minimize nozzle clogging errors. It is an important process error that affects both geometrical accuracy and mechanical properties. Different sensors were used to detect print failures. The study found that monitoring the current of the filament extruding motor helped in the identification of clogging in the FDM process. The authors also proposed a theoretical model.

Mohamed et al. [11] noted that parts with high flexibility could be constructed using a fused deposition additive manufacturing process. They stated that part quality always depended upon the influence of optimum process parameters, an aspect which has not been addressed by the traditional manufacturing process. To create a nonlinear relationship between the accuracy of parts and process parameters, a mathematical model was developed using the I-optimality criterion technique. The obtained results confirmed that the proposed method was found to be highly accurate when compared to the existing normal technique. Dey et al.[12] found that parts produced using the FDM method had poor mechanical properties, inferior surface finish quality and longer build time. By identifying the optimum process parameters, the build time could be reduced. Particle swarm optimization is a technique that is based on experimental values. Thickness, orientation, temperature, and density of process parameters were seen to have an influence on the compressive strength of the product. Kamal et al. [13] studied Polylactic acid (PLA) composite with carbon fiber reinforcement using the FDM method. TOPSIS with analytical hierarchical process-based weightage of a parameter was used to optimize the tensile strength and impact strength. Raj and Prabhu [14] presented the experimentation of the electric discharge machining process with Carbon Nanotube (CNT)-based copper nanoelectrodes and the performance index of material removal rate (MRR). Electrode wear rate (EWR) and surface finish were optimized using TOPSIS multi-objective technique. Ambigai et al. [15] established a fuzzy logic model to analyze the rate of heat transfer for the developed nano and hybrid composites. They also estimated the rate of wear of aluminum graphite reinforced with Si3N4 hybrid composite with better / more accuracy and with fewer prediction errors [16]. Muller et al.[18] reported that the effect of infill density was evident from the gathered/obtained results of their study. There was a decrease in layer height with an increasing infill density value. At 100% infill density, the highest fatigue tensile strength was achieved.

From the comprehensive literature review, it is clear that the Gyroid infill pattern provides higher strength for the component. Process parameters like print and bed temperature, layer height, and infill density directly influence print quality. Warpage and shrinkage phenomena are influenced by the temperature distribution of the deposited layers. Appropriate placement of sensors helps in collecting data and performing real-time process monitoring. Components with large and complex geometries tend to have poorer quality due to the longer interlayer time, which results in poor adhesion of layers. The extensive literature survey reveals that 3D printed complex geometries tend to have poorer quality due to

the prevalence of thermal defects, namely shrinkage and warpage. With the increasing popularity of 3D printing technology in a wide variety of applications and the expansion of its usage from simple prototypes to functional parts, it is vital to understand the magnitude of possible thermal defects. In this study, the defects are considered for three primitive solid geometries during the process of fused deposition modelling. These shapes are the basic solid three-dimensional units used in most modern-day objects. The study of shrinkage and warpage effects on the basic shapes will facilitate a broader understanding of the integrity of complex shapes made employing FDM.

EXPERIMENTAL WORK

Defects in FDM are a result of deformation of the printed component in the form of warpage and shrinkage phenomenon. The present research aims to regulate the effect of printing temperature on the FDM process and address the problems of material warpage and shrinkage by using collected data to build a predictive model. An experimental study is conducted on the process parameters of FDM to design and print components of varying basic geometries with the same volume using the FDM process. The data acquisition of process conditions is done using real-time monitoring techniques incorporating industry 4.0 and recent advancements. Perform data acquisition of process conditions using real-time monitoring techniques incorporating industry 4.0 and recent advancements. The quality of the FDM printed components is determined by checking the warpage and shrinkage values using a coordinate measuring machine (CMM) and Machine Vision. It is observed that the warpage and shrinkage depending on the process parameters. Temperature data-driven models are developed for varying geometries to predict the quality of the component and gain an understanding of the dependence on processing conditions. This experimental study is aimed at obtaining insights into the defects which occur in simple solid geometries.

The control factors in the experiment are varied and have two levels. The values of the factors are decided based on the extensive literature survey and depending on the constraints of the IONIC 3DP Epsilon FDM Printer. The control factors selected for the present study are listed below :

i. Layer thickness: It is a quantification of layer height after consecutive deposition of Polylactic acid (PLA) material over the layers or the print bed, which is the Z-axis vertical resolution. A low value of layer thickness tends to result in a better quality of printed parts along with a smoother surface finish. The drawback of this is longer print times. The two levels of layer thickness selected are 0.2 mm and 0.3 mm.
ii. Print speed: It is the speed at which the printer motor moves the nozzle during the extrusion of the filament. It is inversely related to the print time involved. Extreme levels of print speed result in defective components. Low print speed can cause nozzle clogging and result in deformation due to the excess deposition of the filament at a point. High print speeds can cause deformations mainly because of insufficient and uneven cooling. The result might be the under-extrusion of filament and weak adhesion between layers. The print speeds chosen are 50 mm/s and 80 mm/s.
iii. Infill percentage: It is the volume covered percentage with a printed filament inside the FDM component. The infill percentage is directly proportional to the weight and strength of the component. A higher percentage leads to the greater structural integrity of the component. However, it also tends to increase the print time significantly. The infill percentage values chosen are 20% and 30%, as shown in Table 1.

Table 1. Main effect factors and their values of FDM

Sl.No.	FDM parameters	Units	Quantity of the parameter	
			1	2
1	Layer thickness	m	0.0002	0.0003
2	Print speed	m/sec	0.050	0.080
3	Infill percentage	%	20	30

The density of the pattern is referred to as the infill percentage. 3D-printed parts are typically not produced with a solid interior. Instead, the printing process uses a crosshatch or some other pattern for interior surfaces. This greatly reduces cost due to reduced material usage and print time while moderately reducing strength. The best infill percentage based on the requirements of parts manufactured using FDM is between 20-40% for light-use parts. For functional parts which will undergo some force, a moderate level of infill provides nearly the same strength as a solid part at a reduced cost. 40-100% infill percentage is used for heavy-use parts, and 0-20% is used for non-functional parts.

The objective of building a predictive model in this study is to develop a framework for estimating the defects in FDM. A better understanding of the impact of input variables on the quality of products will be gained. The study aims to provide an approximation by way of an analytical model to determine the range of shrinkage and warpage along with a means to quantify the reliance of defects on temperature variation when basic geometry is printed. Multiple Linear Regression (MLR) models are one of the most prevalent predictive models. The model is used to predict future responses of dependent variables from the pool of collected values of independent variables, along with an equation that explains the relation between them. MLR also determines the contribution of each independent variable to the total variance.

A4 (210×297 mm) paper of 80 gsm size is chosen. The IONIC 3DP printer has 4 Allen keys which control the z-movement of the print bed. The Allen keys are located at the corners of the printer. The printer has preset test coordinates for leveling the print bed. It is assumed that the coordinate system has points [(1,1),(1,-1),(-1,1),(-1,-1)] on the printer bed

where the center of the bed is the origin. The printer head is moved to (1,1) while making contact with the print bed, and an A4 paper is placed under the nozzle. The Allen key is adjusted in the z-axis movement until a slight resistance is felt while the A4 sheet is moved. The main calibration criteria to avoid is easy movement of paper (the nozzle could be far) or no movement of paper at all (the nozzle could be too close). The same process is repeated for other coordinates [(1,-1),(-1,1),(-1,-1)]. This process is repeated completely two times to increase the accuracy of calibration. Failure to calibrate the print bed causes an uneven bed which in turn results in loss of filament, energy and time spent to heat the print bed. The ends of the fiber optic sensors are connected to the channels present in the screw terminal connectivity region. The NI DAQ USB-6002 has the functionality of self-calibration, which is guaranteed for two years. The self-calibration function has the ability to characterize non-linearity, gain and offset errors in the device. The precision of the fiber sensor is checked by measuring the print bed temperature of the IONIC 3DP. The printer has a display which indicates the print bed temperature. It must be ensured that the measured signals are in accordance with displayed temperature readings.

Selection of Material

There are various kinds of materials that are used for FDM processes, such as PLA material, Acrylonitrile Butadiene Styrene (ABS) material, stereolithography materials (epoxy resins), polyamide (nylon), etc. PLA and ABS are the most common materials used in these processes because of their lower costs and easier availability. Mechanical properties like flexural modulus, the tensile strength of the material, and elastic modulus of ABS are much higher than PLA, but it is much harder to print compared to PLA. The major advantage of PLA is that it is best suited to print components requiring intricate details because of its lower printing temperatures compared to other thermoplastics.

The experiment is conducted to study the quality of the printed FDM components under the selected processing conditions. PLA is found to be a more suitable material for studying the warpage and shrinkage phenomenon. For studying the thermal defects that occur in the FDM process, three primitive solid geometries with the same volume are chosen to be printed. These shapes are the basic solid three-dimensional units used in most modern-day objects. The study of shrinkage and warpage effects on the basic shapes will facilitate a broader understanding of the integrity of complex shapes made employing FDM. The Computer Aided Design (CAD) modelling for these shapes is done using Solid works 2018, as portrayed in Figure 1. PLA material is utilized for printing the components in this experiment. Ensuing studies on FDM can focus on the variation in the finished quality of components when ABS and other such materials are used, as depicted in Figure 2. The experimental study also introduces the use of a Data Acquisition (DAQ) module for real-time temperature monitoring which is coupled with a fiber optic sensor. This, along with findings of the impact of thermal data on defects, provides a framework for the set up of a data acquisition system and for the collection and quantification of temperature data gathered during the printing process

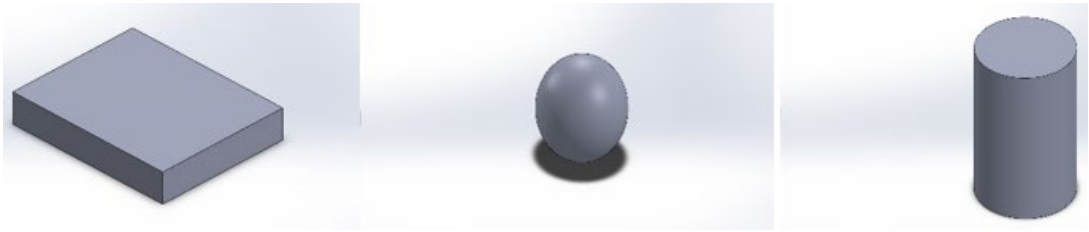

Figure 1. 3D solid models of rectangle, sphere and cylinder

The experimental study requires the use of three control factors, namely, Layer Thickness (factor A), Print Speed (factor B), and Infill Percentage (factor C). Each factor has two levels represented by '1' for the low-level setting and '2' for the high-level setting, as shown in design Table 1. The 2^k full factorial design is extensively used to design experiments with two levels and several factors. Since the experimental work consists of three factors, that is k=3, a full factorial 2^3 design with two replicates are used for 8*1=8 runs per solid geometry. Factorial design with all possible combinations of the experiments is done using Minitab 17 software. The time taken to fabricate the different models using FDM is shown in Table 2.

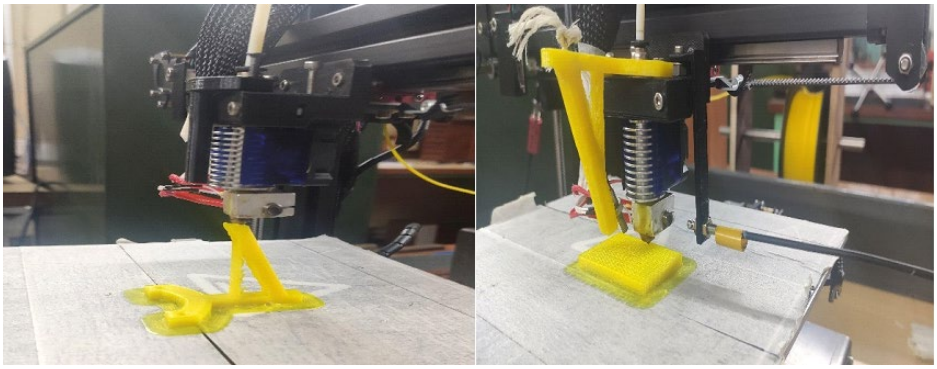

Figure.2 Experimental FDM model manufactured Print bed fixture with assembly

Table 2. FDM model fabrication time duration

Exp.No.	Layer thickness (m)	Print speed (m/sec)	Infill percentage (%)	Time taken to print (min)		
				Cuboid	Cylinder	Sphere
1	0.0002	0.050	20	65	62	63
2	0.0002	0.080	20	47	49	50
3	0.0002	0.050	30	42	41	40
4	0.0002	0.080	30	59	51	48
5	0.0003	0.050	30	30	29	27
6	0.0003	0.080	30	47	45	44
7	0.0003	0.050	20	80	72	68
8	0.0003	0.080	20	43	36	32

Fiber optic temperature sensors are non-conductive sensors used to measure temperature and are based on the fundamental principle of photovoltaic effect. The fiber optic sensors are used to monitor the temperature changes in the layer-by-layer deposition of the component; the captured signals are sent to the DAQ through appropriate channel wiring which is visible in the LabVIEW, as depicted in Figure 3. The study also examines/considers the impact of temperature profile across layers on the experimentally calculated defects by showing the relative considerable contribution of thermal gradient through an ANOVA table. Moreover, the study finds that the thermal gradient is directly proportional to the experimental shrinkage (%) and warpage (%) calculations with the exception of height shrinkage (%) for cuboid. The cause for this anomaly is also discussed.

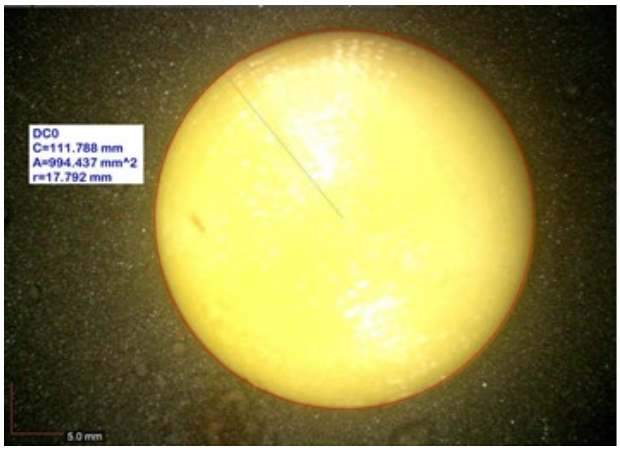

Figure 3. Measurement of circle using machine vision

The NI Data Acquisition Hardware coupled with DAQ compatible fiber optic sensor is used to collect data for the purpose of temperature measurement. DAQ is connected to the PC with USB 3.0 to monitor signals in LabVIEW software. Machine vision is used for measuring sphere components by fitting a circle with 10 points. Since the distortion is high in the sphere due to single-contact printing without supports, this method is used to validate and cross-check the dimensions of the sphere. The sphere geometry ideally has an equal diameter in all directions. The measured diameter through microscope imaging tends to have variations which occur during the FDM process. The variation between the design diameter and measured diameter characterizes the warpage of the sphere.

RESULTS AND DISCUSSION

After the experimental study is performed, the data collected from the testing equipment is given as input to the formulae mentioned in Eq. (1) to (3). The results generated for each solid geometry are given in Table 3. The temperature gradient is calculated based on the interlayer heat distribution with different heights of the layer thickness. There is a difference between the temperature of the maximum layer and the temperature of the minimum layer. FDM model accuracy depends upon the dimensional accuracy of the cylinder parts manufactured, which greatly affects the shrinkage problem. Minimizing and optimizing the shrinkage of the material is essential to obtain good quality products. The diameter difference is measured based on the design diameter and the mean of the diameter measured by the CMM. The design diameter used here is 31.91 mm. Similarly, height shrinkage is based on the height difference between the parts. The height diameter used is 25 mm. Warpage defects have to be minimized by using less layer thickness because it doesn't make the part more resistant to bending. Interlayer wait time and other continuous factors related to the FDM process can be included in combination with a temperature gradient to achieve a predictive model with a higher R square value which gives a better fit to the experimental data.

$$Temperature\ gradient\ = \left(\frac{Temperature\ \ difference}{Design\ height\ of\ component}\right) \quad (1)$$

$$Diameter\ shrinkage\ (\%) = \left(\frac{Diameter\ difference}{Design\ diameter}\right) \times 100 \quad (2)$$

$$Warpage = \frac{\sum_{i=1}^{3}(\ Maximum\ probe\ travel_i\ - Minimum\ probe\ travel_i\ )}{3} \quad (3)$$

Table 3. Shrinkage and warpage characteristics of different FDM model

Exp. no.	Cuboid			Cylinder			Sphere		
	Temperature gradient (K/mm)	Shrinkage (%)	Warpage (%)	Temperature gradient (K/mm)	Shrinkage (%)	Warpage (%)	Temperature gradient (K/mm)	Shrinkage (%)	Warpage (%)
1	273.63	1.4912	0.5398	273.50	3.682	0.7134	273.54	1.362	0.381
2	273.68	1.338	0.1276	273.61	2.544	0.7091	273.69	1.611	0.299
3	273.42	1.347	0.0881	274.24	2.759	0.7858	273.55	1.937	0.156
4	273.69	1.435	0.2001	274.34	2.391	0.4372	273.49	1.822	0.325
5	273.80	1.990	0.3360	273.87	4.028	0.3724	273.62	1.461	0.190
6	273.81	1.115	0.0854	273.66	3.154	0.7305	273.76	1.203	0.444
7	273.72	1.074	0.1907	273.77	3.429	0.4678	273.69	1.706	0.758
8	273.80	1.753	0.1131	273.64	2.925	0.5160	273.59	1.697	0.554

Regression Analysis

Linear regression analysis is a preferred Machine learning (ML) algorithm. It is a statistical technique that is widely used for the prediction of the process for continuous variables, real variables, and numeric values such as cost, time, and price. Linear regression gives the linear or straight relationship between output variables (y) and input variables (x). It gives a linear relationship, which means that the dependent variable fluctuates according to the independent output variable. The accuracy of the regression models can be increased by performing a higher number of replicate runs in the experiments. The empirical model is:

$$Y = A(X_1)^a(X_2)^b(X_3)^c(X_4)^d \quad (4)$$

where, Y is shrinkage or warpage response (%), A is coefficient, X_1 is temperature gradient (°C/mm), X_2 is layer thickness (mm), X_3 is print speed (mm/sec), and X_4 is infill percentage (%). The regression model for each output variable is constructed from the experimental data for future prediction of responses. The equation explains with the help of coefficients, how an increase of one unit in each factor causes a change of units equal to their respective coefficients in the response when other factors remain the same.

Through the predictive model, regression equations are generated to determine the shrinkage and warpage defects on basic shapes using common process parameters (Layer Thickness, Print Speed, Infill Percentage) within the established range for FDM. The equations can be used to obtain values for the defects in these shapes when similar process parameters are used for 3D printing using FDM. The equations also provide coefficients for each process parameter. These coefficients are the amount by which the shrinkage and warpage values increase for a unit increase in the process parameter, other factors remaining constant. For cuboid,

$$Length\ shrinkage\ (\%)\ =\ 1.6 + 0.08 * X1 - 0.552 * X2 + 0.07 * X3 + 0.231 * X4 \quad (5)$$

$$Breadth\ shrinkage\ (\%)\ =\ 0.826 + 0.117 * X1 - 0.071 * X2 + 0.261 * X3 + 0.06 * X4 \quad (6)$$

$$Height\ shrinkage\ (\%)\ =\ 4.23 - 1.51 * X1 - 0.31 * X2 + 0.548 * X3 - 0.421 * X4 \quad (7)$$

The results of the multiple linear regression model in the experimental study reaffirm the dependence of warpage on the temperature profile between layers which is quantified as a thermal gradient. From the ANOVA analysis, it is found that the thermal gradient in the sphere and cylinder contribute 9.2% and 15.23%, respectively to the variation in the warpage defect. The factorial plots and the regression equation confirm a positive correlation between the thermal gradient and warpage of the sphere and cylinder. The coefficients in the equation are 1.25 for sphere and 0.64 for cylinder, respectively. This implies that for every 1 unit increase in the thermal gradient (°C/mm), the warpage of sphere and cylinder increases by 1.25 mm and 0.64 mm, respectively. The significance level considered in this study is $p<0.05$. This positive trend between the predictor and the response shows that the considerable variation that occurs is an increment in warpage with an increase in the thermal gradient.

ANOVA analysis for Cuboid FDM model

Significant factors cannot be tested using Analysis of Variance (ANOVA), but the empirical prediction model can be obtained using Regression Analysis. This technique compares the main effect factor and effect due to noise factor using ANOVA. F-tests are obtained from the variance calculation. It is used to understand the contribution of individual factors to the total variance. The results of ANOVA are displayed in Table 4 and show that the layer thickness has a large contribution of 48.27% to the variance of length shrinkage followed by print speed of 21.98%. An F-value of 19.12 for layer thickness indicates significant changes in the length shrinkage, and a large F-value indicates a better model which fits the data very well in FDM products. Similarly, the layer thickness has the most significant contribution to the variance of breadth shrinkage with a percentage contribution of 70.41%. An F-value of 145.21 for layer thickness indicates that there are significant changes in the breadth shrinkage.

Table 4. ANOVA analysis of length shrinkage and height shrinkage in cuboid of FDM model

	Factors	Degree of freedom (f)	Sum of square (SS_A)	Adjusted Ms	F-Value	P-Value	Contribution (%)
Length shrinkage	Temperature gradient (°C/mm)	1	0.117	0.117	2.85	0.340	7.2
	Layer thickness (mm)	1	0.784	0.784	19.12	0.143*	48.27
	Print speed (mm/sec)	1	0.357	0.357	8.70	0.208	21.98
	Infill percentage (%)	1	0.243	0.243	5.92	0.248	14.96
	Error	3	0.124	0.041			7.63
	Total	7	1.624	*Significant			
Height shrinkage	Temperature gradient (°C/mm)	1	0.4728	0.4728	42.98	0.0963	20.84
	Layer thickness (mm)	1	1.5974	1.5974	145.21	0.05*	70.41
	Print speed (mm/sec)	1	0.1129	0.1129	10.26	0.192	4.97
	Infill percentage (%)	1	0.1377	0.1377	12.51	0.175	6.07
	Error	3	0.0332	0.011			1.46
	Total	7	2.2682	*Significant			

Factor Effect Diagram on Cuboid FDM Model

The main effect factorial plot, as depicted in Figure 4, is used to examine each factor's influence on the response. The fitted means of the response data are plotted against the factors. Through this, the relation trends between each input variable and output variable are observed to determine whether the high level or low level of a controlling factor causes excessive defects. Response values are predicted by inputting the various combinations of factors into the regression equation obtained through the multiple linear regression analysis. These predicted response values are then plotted against their corresponding experimental response values in a scatter plot with a regression line. Further, a relationship is established between the predicted and experimental response values. This relationship is expressed in the form of a regression equation. The solution identifies the best combination of factors, which involves choosing the optimal level (high/low) for the control factors, namely layer thickness (mm), print speed (mm/sec), and infill percentage (%) along with a value for temperature gradient (°C/mm) that jointly optimize the fitting response.

Along with this combination, a response value is generated, which satisfies the optimization aim. In the present experimental study, the goal is to minimize the shrinkage (%) and the warpage (%) for each solid geometry. Subsequent studies can aim at experimentation in a controlled environment with a closed chamber instead of ambient conditions like those in the current study. The difference in responses will help gain a better understanding of the shrinkage and warpage phenomenon. The optimal solution is obtained based on the factor effect diagram, as depicted in Table 5.

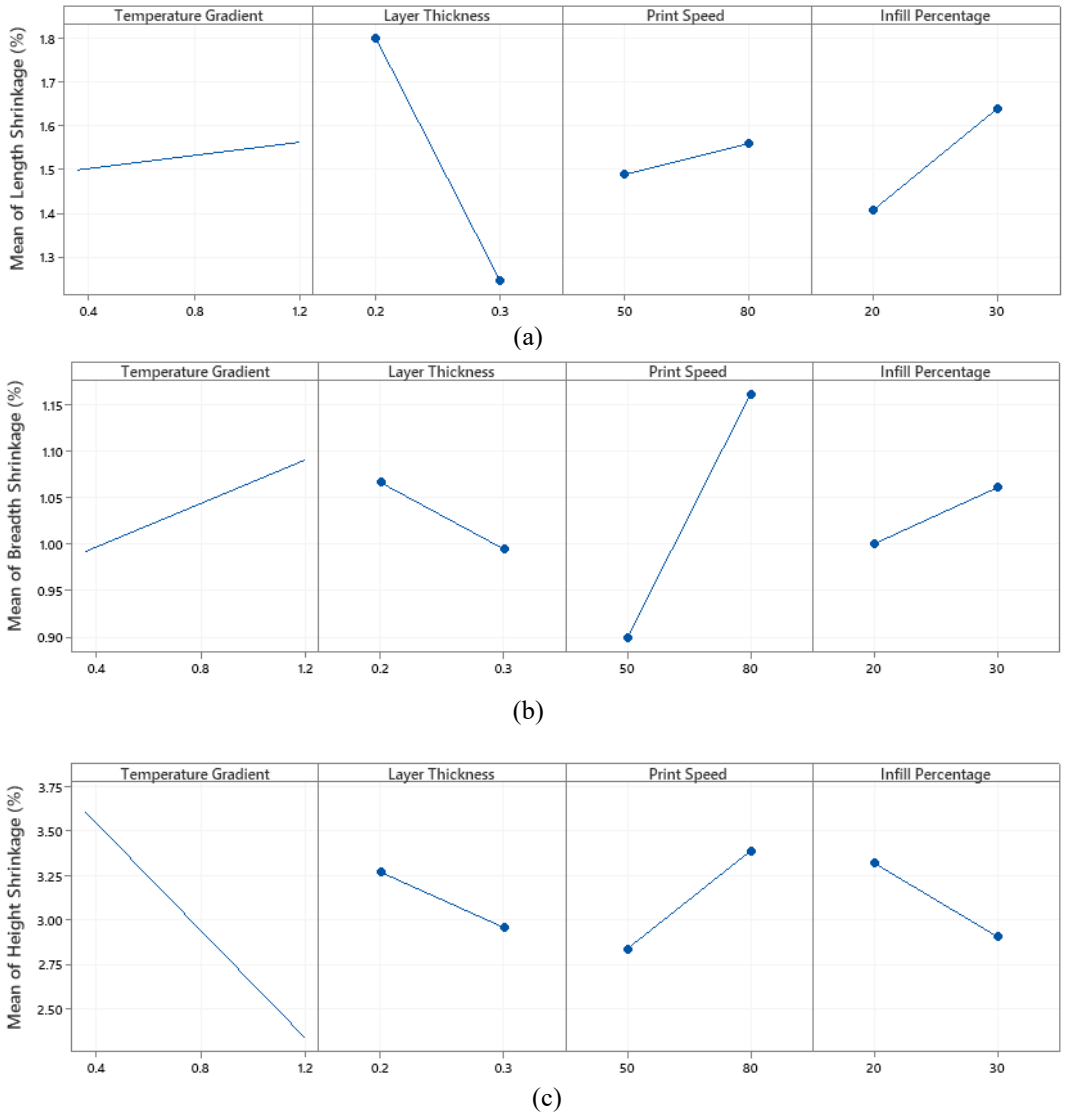

Figure 4. Factorial plot of (a) length shrinkage, (b) breath shrinkage and (c) height shrinkage in cuboid for FDM model

The factorial plots for defects in all three shapes show the relationship between each process parameter and the response and the level (for categorical factors) at which the defect is least. This relation is used to input the factor values into the regression equation accordingly to get an optimized solution. The optimized solution for each shape will help in minimization of defects.

Table 5. Optimized solution for cuboid model of FDM

Layer thickness (m)	Print speed (m/sec)	Infill percentage (%)	Length shrinkage (%)	Breath shrinkage (%)	Height shrinkage (%)
0.0003	0.050	20	1.072	0.937	0.755

TOPSIS Method for Cuboid FDM Model

The TOPSIS method is one of the two objective optimization methods where the positive hypothesis and worst solution negative hypothesis are also considered [17].

Step 1: The objective function is finalized

Step 2: The analytical hierarchy process? (AHP) is portrayed. Table 6 shows the importance of each criterion. The first row is assigned to the first parameter of FDM, and each column represents a particular response.

Step 3: The following Eq. (8) is used to normalize the different response units r_{nm} :

$$r_{nm} = \frac{x_{nm}}{\sqrt{\sum_{n=1}^{k} x_{nm}^2}} \tag{8}$$

Step 4: The normalized response values are multiplied by the weightage of individual response given in Table 7.

$$GN_m = \left[\prod_{m=1}^{p} a_{nm}\right]^{1/N} \tag{9}$$

$$W_j = GN_m / \sum_{m=i}^{Q} GN_m \tag{10}$$

Table 6. Matrix AHP table for circle type FDM model [14]

Criteria	Temperature gradient (K/mm)	Shrinkage (%)	Warpage (%)
Temperature gradient (K/mm)	1	3	2
Shrinkage (%)	1/3 (0.33)	1	½ (0.5)
Warpage (%)	1/2 (0.5)	2	1
Sum	1.83	6	3.5

Table 7. Weightage of individual response table

Experiment number	Temperature gradient (K/mm)	Shrinkage (%)	Warpage (%)
Weightage	0.539	0.163	0.297
1	0.4857	1.4912	0.5398
2	0.5311	1.3380	0.1276
3	0.2772	1.3468	0.0881
4	0.5437	1.4350	0.2001
5	0.6541	1.9902	0.3360
6	0.6594	1.1148	0.0854
7	0.5772	1.0740	0.1907
8	0.6550	1.7532	0.1131

Pairwise Comparison Matrix

To make the intensity-based best decision, a highly beneficial tool is proposed to hierarchize the criteria. The data in the normalized decision table and the criteria weights are compounded to create the weighted normalized Table 8 and Table 9 are obtained as temperature gradient(°c/mm)= 0.539, shrinkage (%)= 0.163, and warpage (%) = 0.297 by Eq. (9) and Eq. (10).

Step 5: The desired and non-desirable solutions are calculated and summarised,

$$(\text{Vnm.})\ \text{Vm} = \text{Wnm rnm} \tag{11}$$

To get the weighted normalized table, the data in the normalized decision table and the criteria weights are multiplied.

Step 6: Using Eq. (12) and Eq. (13), the desirable and non-desirable solutions are calculated and tabulated in Table 10.

$$V^{+} = \{[\sum_{n}^{Max} V_{nm}\ /m\epsilon\ M], [\sum_{n}^{Min} V_{nm}\ /m\epsilon\ M]\ /1,2..K\} \tag{12}$$

$$V^{-} = \{[\sum_{n}^{Min} V_{nm}\ /m\epsilon\ M], [\sum_{n}^{Max} V_{nm}\ /m\epsilon\ M']\ /1,2..N\} \tag{13}$$

M = (m= 1,2,...,K)/m is connected with attributes that positively contribute, while M'= (m = 1,2,...,K)/m is related with attributes that do not have a positive contribution.

Table 8. Pairwise correlation matrix

Criteria	Temperature gradient (K/mm)	Shrinkage (%)	Warpage (%)	Criteria weight
Temperature gradient (K/mm)	1/1.83	3/6	2/3.5	0.539
Shrinkage (%)	0.33/1.83	1/6	0.5/3.5	0.163
Warpage (%)	0.5/1.83	2/6	1/3.5	0.297
Sum	1.83	6	3.5	

Table 9. Calculating the consistency

Criteria	Temperature Gradient (K/mm)	Shrinkage (%)	Warpage (%)	Weighted sum values	Criteria Weight	
Criteria Weight	0.539	0.163	0.297			
Temperature Gradient (K/mm)	1*0.539	3*0.163	2*0.297	1.622	0.539	3.009
Shrinkage (%)	0.33*0.539	1*0.163	0.5*0.297	0.489	0.163	3.000
Warpage (%)	0.5*0.539	2*0.163	1*0.297	0.892	0.297	3.005

Step 7: The following formula is used to determine how close a certain choice is to the ideal solution:

$$P_i = S_n^- / (S_N^+ + S_n^-) \quad (14)$$

Step 8: The set of options is sorted in decreasing order, with the most preferred and least preferred responses designated by the Pn value. Equation (14) calculates the relative contiguous co-efficient (Cn*) of FDM, as shown in Table 10 and Table 11.

Table 10. Weighted normalized table

Exp. No.	Temperature gradient (K/mm)	Shrinkage (%)	Warpage (%)
Weightage	0.539	0.163	0.297

Table 11. Most preferred and least preferred responses and contiguous co-efficient (Cn*) FDM

Exp. No.	S_n^+	S_n^-	C_n^*
1	0.177773	0.138727	0.438316
2	0.082408	0.212173	0.720254
3	0.210752	0.170283	0.446896
4	0.092261	0.197490	0.681586
5	0.166884	0.211975	0.559508
6	0.006650	0.284626	0.977168
7	0.054232	0.243310	0.817734
8	0.118671	0.242940	0.671827

Table 12. S/N Ratio response larger is better for closeness co-efficient (Cn*)

Level	Layer thickness (mm)	Print speed (mm/sec)	Infill percentage (%)
1	-5.085	-5.238	-3.804
2	-2.612	-2.459	-3.892
Delta	2.473	2.779	0.088
Rank	2	1	3

In FDM experiments, the mean S/N ratio is calculated based on the larger, the better response, as portrayed in Table 12. Based on the values, it is seen/observed that the most favored multi-response combination is with 0.3 mm thickness of the object layer, when the printing speed is 80 mm/sec and the percentage of materials infilled in an object is 30%, specified as A2B2C1. For the circular object model, the predicted factorial design analysis-based values are temperature 0.6541°C/mm, shrinkage 1.99%, and warpage 0.336%. Figure 5 portrays the longer length parameter of printing speed as the most influencing parameter for FDM model fabrication. The confirmation experiments are conducted based on A2B2C1 optimum parameters and it is reaffirmed that the predicted factorial response and experimental closeness coefficient errors are minimum, with an acceptable range of less than 10%.

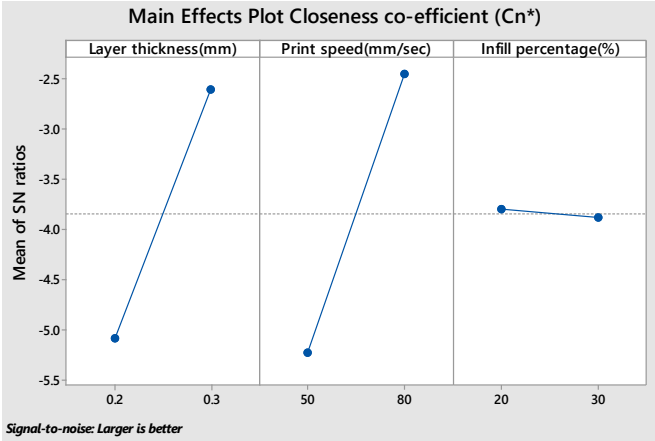

Figure 5. Factor effect diagram for relative closeness of FDM process

The results given in Table 12 indicate that the layer thickness (55.60%) has a significant influence while the print speed (33.16%) has a lesser influence on the FDM model temperature gradient values for the contiguous co-efficient (Cn*).

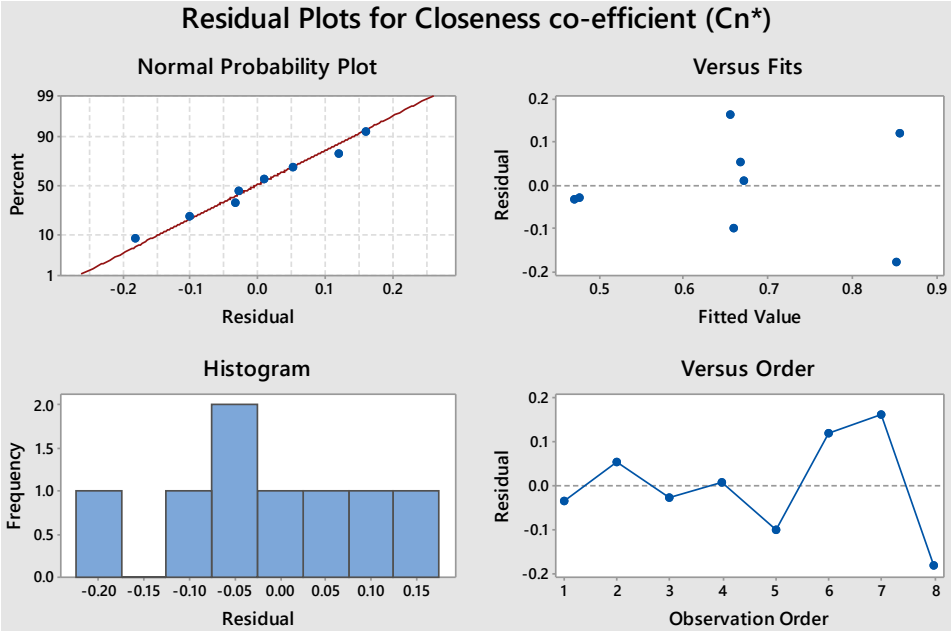

Figure 6. Observed and fitted response Plots for Cn*

Observed and fitted response plots, as portrayed in Figure 6, show how much the linear line deviated from the data points for fitting the experimental values, and the outliers of the data points can be identified. The residual values are fitted on the vertical axis, and the independent coefficient (Cn*) is on the horizontal axis. The residual values must be randomly and uniformly distributed around the regression line. Here, interaction terms are not able to identify the effect on the FDM process. The likeness between experimental and predicted values is R2= 0.923, which explains the 92.3% of total accuracy after removing outliers. In Table 13, the ANOVA analysis is summarized, and a numerical framework is proposed. After taking into account the notable factor of layer thickness, the proposed structure describes the entire variability, and the second contributing parameter is identified to be print speed.

Table 13. ANOVA analysis using TOPSIS ranking results

FDM Factors	DOF	SS_A	V_A	FA_o	P	Contribution (%)
Layer thickness (mm)	1	0.128299	0.068299	4.10	0.153	55.60
Print speed (mm/sec)	1	0.077693	0.077693	3.52	0.134	33.16
Infill percentage (%)	1	0.00036	0.000036	0.00	0.970	0.153
Error	4	0.028201	0.022050			11.96
Total	7	0.234229				100

Note: Significant; S=0.1484 R-sq = 92.34% R-sq(adj)= 34.10%

Confirmation Test

Implementation of any optimization technique and predictions need to be cross-verified by carrying out the confirmation test. Hence, the relevant test is carried out and presented in Table 14. The temperature gradient obtained is 0.6594 °C/mm while the initial value is 0.4867 °C/mm with the operational parameters of layer thickness 0.3 mm, print speed 80 mm/sec, and infill percentage 20%. The most advantageous characteristics and an increase in layer thickness imply that TOPSIS multi-criteria decision-making produces the most favorable design, improving the experimental and predicted results.

Table 14. Results of confirmation tests for cylinder part of FDM [14]

	Initial FDM experiment Design	Optimal FDM predicted design	
		Prediction	Experiment
Setting level	A1B1C1	A2B2C1	A2B2C1
Temperature Gradient (K/mm)	273.63	273.80	273.81
Shrinkage (%)	1.4912	1.9902	1.9148
Warpage (%)	0.5398	0.3360	0.3854
Closeness coefficient	0.4383	0.579	-

FUZZY LOGIC ANALYSIS

Fuzzy Logic Analysis is used to determine the correlation between cylinder shrinkage as output response and layer thickness, print speed, and infill percentage as input process variables. The fuzzy process goes under fuzzification, which converts crisp input into fuzzy variables. The fuzzy logic, if then else rules are implemented to convert them into new fuzzy numbers. The input variable has three triangular membership functions of layer thickness [0.2-0.3], print speed [50-80], and infill percentage [20-30]. The output membership functions of shrinkage [2.4-4] are depicted in Figure 7.

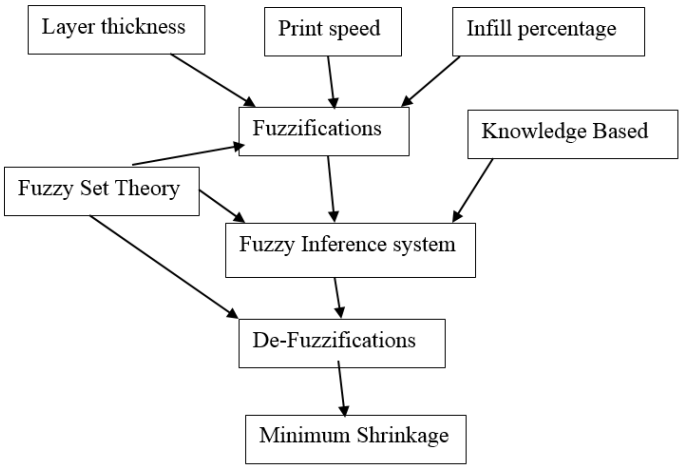

Figure 7. Schematic representation of the Fuzzy algorithm for FDM

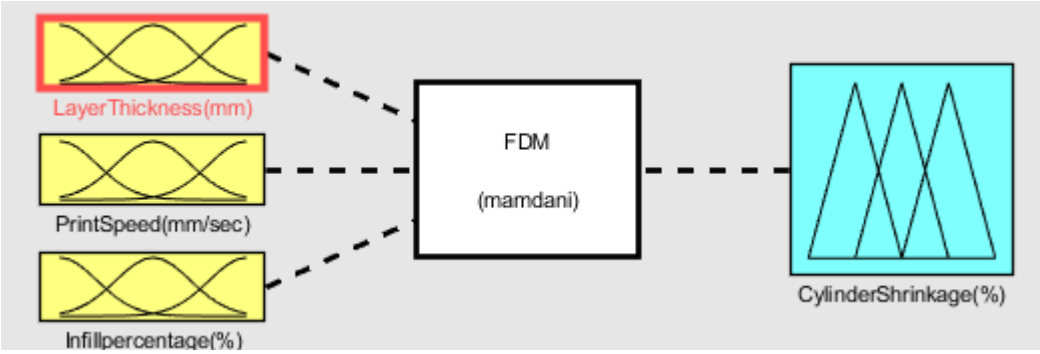

Figure 8. Membership functions of FDM

Input parameters of layer thickness, print speed, and infill percentage of three different zones of membership functions are selected based on inputs given by machining experts and fuzzy logic experts. The row vector of Layer thickness is A= {L, M, H}, where L is 0.2 mm, M is 0.25 mm, and H is 0.3 mm. The degree of membership function of layer thickness, print speed, and infill percentage is depicted in Figure 8, and the output membership function of cylinder shrinkage % is

depicted in Figure 8 with the fuzzy logic function divided into five memberships of S = {VL, L, M, H, VH}, where VL is very low and VH is very high. These values are chosen based on experimental data, as shown in Figure 9.

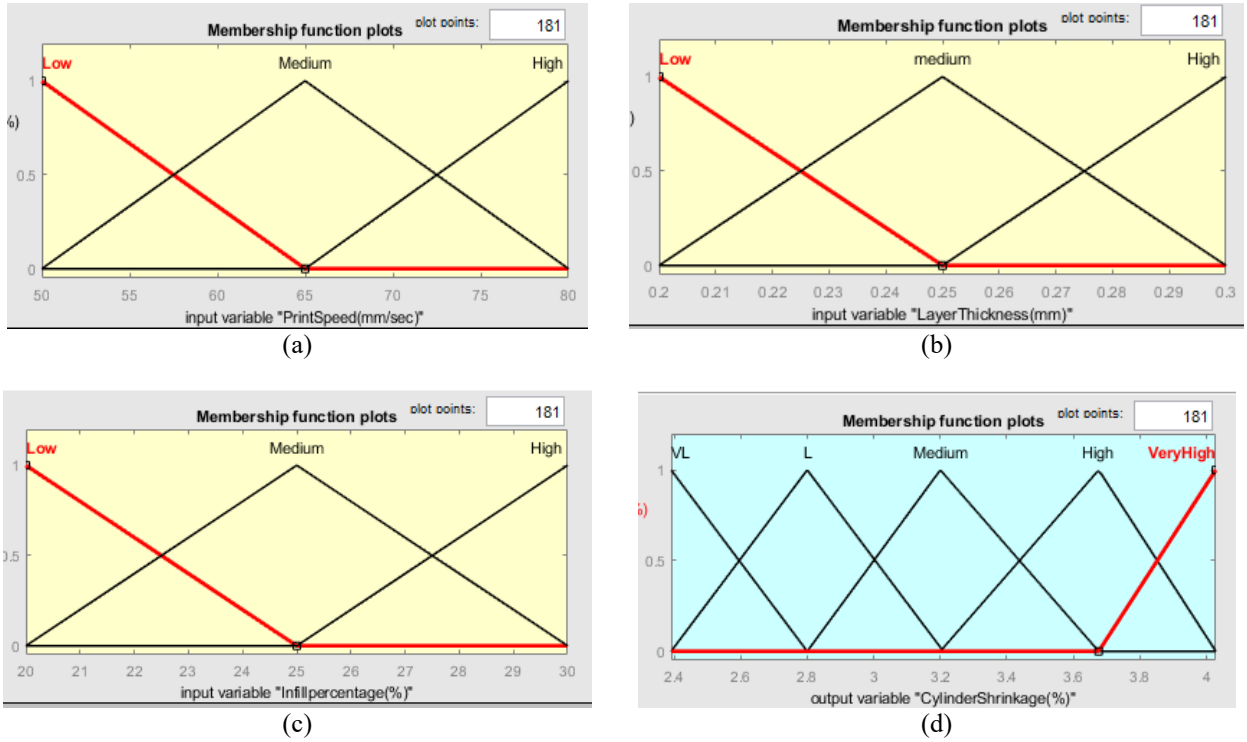

Figure 9. Input membership function of (a) print speed, (b) layer thickness, (c) infill percentage and (d) output membership function of cylinder shrinkage

The membership function of layer thickness (mm) in equation form is listed as follows:

$$L_1(x) = \frac{0.25 - x}{0.05}, x \in (0.2, 0.25) \tag{15}$$

$$L_2(x) = \begin{cases} (x - 0.3)/0.05 \\ (0.25 - x)/0.05, \end{cases} x \in (0.2,0.25) and\ x \in (0.25,0.3) \tag{16}$$

$$L_3(x) = \frac{x - 0.3}{0.05}, x \in (0.25,0.3) \tag{17}$$

Table 15 defines the fuzzy rule matrix, which is used in this study of shrinkage allowances of cylinder components made by fused deposition modeling. The number of rules is fixed depending upon the number of. Here, the total number of the rule set defined for this system is 9. Primarily, fuzzy rules influence the relationship between input FDM parameters and output shrinkage %, which permits the exact cylinder material selection according to the centroid method of area-based defuzzification. The fuzzy rules can be expressed by Eq. (18). Input parameters are used as three levels, and the output responses are divided into five levels to ensure the accuracy of the response using the fuzzy logic analysis.

$$F(L_i, P_i, I_i) - L(i, j, k)\varepsilon\ [1,3]; p, q, r, s, t\ \varepsilon[1,5]; ij, k, p, q, r, s, t\ )\varepsilon\ z \tag{18}$$

Fuzzy Rules

Fuzzy rules are defined for the above-mentioned system using the output of the machine learning model and the range of values is set based on inputs obtained from machining experts. The data are fed as input and reference for the system to predict the corresponding output value and condition. The total number of the rule set defined for this system is nine.

i. Rule 1: If layer thickness(mm) is low, print speed (mm/sec) is low and infill percentage(%) is low, then cylinder shrinkage (%) is low.
ii. Rule 2: If layer thickness (mm) is low, print speed (mm/sec) is medium and infill percentage(%) is low, then cylinder shrinkage (%) is medium.
iii. Rule 3: If layer thickness(mm) is low, print speed (mm/sec) is high and infill percentage(%) is low, then cylinder shrinkage (%) is high.
iv. Rule 4: If layer thickness(mm) is medium, print speed (mm/sec) is low and infill percentage(%) is low, then cylinder shrinkage (%) is very high.

v. Rule 5: If layer thickness(mm) is medium, print speed (mm/sec) is medium and infill percentage(%) is low, then cylinder shrinkage (%) is medium.
vi. Rule 6: If layer thickness(mm) is medium, print speed (mm/sec) is high and infill percentage(%) is low, then cylinder shrinkage (%) is low.
vii. Rule 7: If layer thickness(mm) is high, print speed (mm/sec) is low and infill percentage(%) is low, then cylinder shrinkage (%) is very high.
viii. Rule 8: If layer thickness(mm) is high, print speed (mm/sec) is medium and infill percentage(%) is low, then cylinder shrinkage (%) is very low.
ix. Rule 9: If layer thickness(mm) is high, print speed (mm/sec) is high and infill percentage(%) is low, then cylinder shrinkage (%) is high.

The fuzzy logic is carried out with the rule base of 9 numbers and the following figures depict the prediction under given conditions. Figure 10 depicts the input parameters in each column with a triangular membership function. It is shown in actuated by yellow color; at a time, more than three rules are actuated and combined to get the output parameter of shrinkage percentage. Combining all the areas of output triangular membership and forms the area-based object and centroid method is used to calculate the single output defuzzification value as depicted in the red color line. All the areas of output triangular membership are combined to form the area-based object, and the centroid method is used to calculate the single output defuzzification value, as depicted in the red color line. Figure 11 indicates that if the layer thickness is increased from 0.24 mm to 0.26 mm, then the shrinkage allowances decrease rapidly. The infill percentage is initially stable up to 25% after which there is a rapid increase in the shrinkage percentage

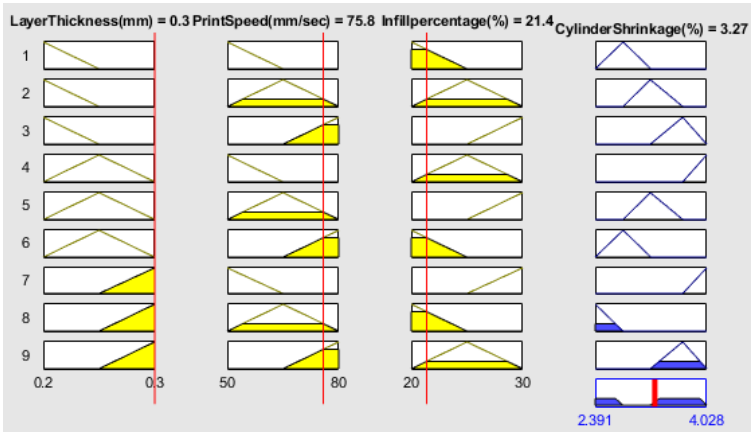

Figure 10. Fuzzy system prediction under cylinder component shrinkage %

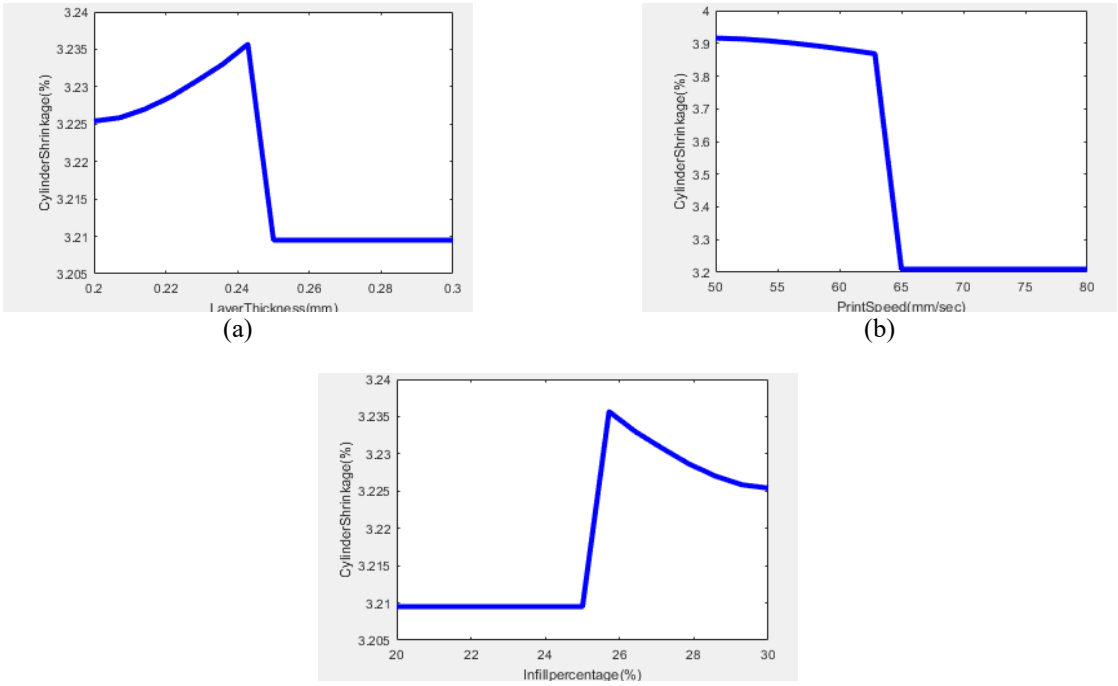

Figure 11. 2D representation of optimum FDM shrinkage: (a) layer thickness vs shrinkage (b) print speed vs shrinkage (c) infill percentage vs shrinkage

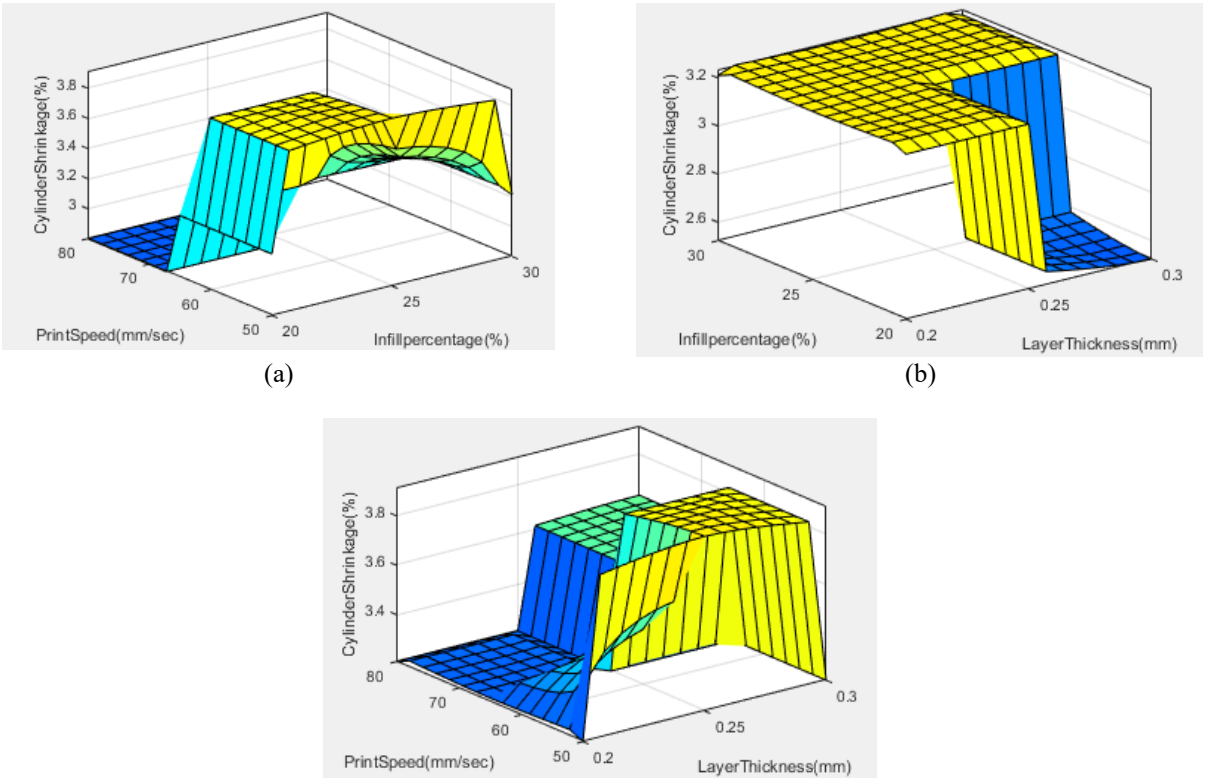

Figure 12. 3D surface plot based fuzzy logic outputs for FDM cylinder shrinkage percentage

The low value of layer thickness tends to result in high shrinkage. On increasing the thickness, the shrinkage decreases due to the stability of the materials, as depicted in Figure 12. Also, if the print speed is increased, then the shrinkage allowances decrease due to the non-availability of solidification time. The infill percentage is uniformly maintained to get a uniform shrinkage %. The infill percentage is directly proportional to the weight and strength of the component. A higher percentage leads to the greater structural integrity of the component, as depicted in yellow color.

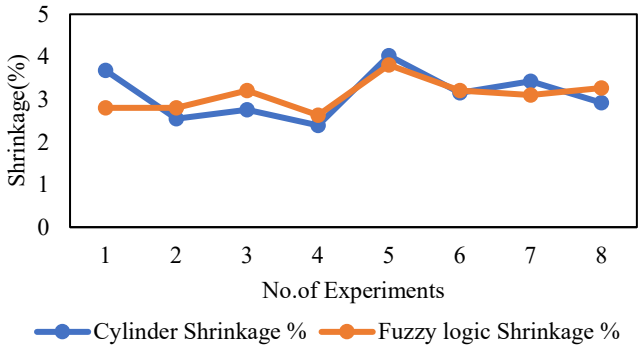

Figure 13. Comparison of experimental and fuzzy logic model of shrinkage percentage

Figure 13 shows the shrinkage % obtained from the fused deposition modeling. The experimental analysis and Fuzzy logic analysis are compared for cylinder components. The fuzzy expert system model is noted to more accurately predict the results with real experimental values, and the model has less than 5% error. These results indicate that no further experimental work is needed to obtain the shrinkage % of a workpiece. This fuzzy expert model will reduce the cost and time of the experiments and predict the result accurately based on experts' knowledge. If there are slight deviations in the results, then the fuzzy rule base system can be modified or deleted so that more than 95% accuracy of predicting the shrinkage allowances can be achieved.

CONCLUSIONS

The FDM model is used to determine the effect of temperature on the aforementioned shrinkage and warpage phenomenon by using collected data to build a predictive model. The goal of the study is to predict the outcome of the defects while establishing a relationship between the process parameters and the response by integrating them into a model. The following research outcomes are identified and implemented in a circular model.

i. The optimal Cn* of coefficient with S/N ratio, for circular model creation in FDM with the process parameter of temperature gradient, is 273.80 K/mm while the initial value is 0.4867°C/mm. The most favorable combinations of the experiment are obtained from the response diagram for the process parameters of layer thickness 0.3 mm, print speed 80 mm/sec, and infill percentage 20%. It is noted that the parameters have a contribution of 55.60%, 33.16%, and 0.15%, respectively.
ii. From the relative closeness coefficient (C*.) obtained from the TOPSIS results, it is concluded that the layer thickness has a high influence while print speed has a low influence on the multiple responses. The residual plots for the relative closeness coefficient (Cn+) show that layer thickness is the most important parameter, which improves the temperature gradient and reduces the shrinkage and warpage.
iii. From the factorial plots, it is apparent that the thermal gradient is directly proportional to experimental shrinkage and warpage calculations except for height shrinkage for the cuboid. The anomaly of height shrinkage of the cuboid can be attributed to the occurrence of peak distortion in FDM components occurring at an intermediate part height, beyond which the increase in thermal effects does not lead to an increase in deformation. The variation in height shrinkage for cuboids has a significant contribution of 20.84% from the thermal gradient.
iv. Predictive models for height shrinkage of cylinder and shrinkage have high R-squared R-Sq. values of 0.622 and 0.80, respectively, showing that the generated regression equation has a good fit with experimental data. The fuzzy expert system model predicts the results more accurately with real experimental values and the error is less than 5%.
v. Thermal gradient significantly influences warpage defects in the sphere and cylinder; a positive correlation is noted with respective contributions of 9.2% and 15.23% to the response variation. Thermal gradient can be considered a useful predictor of warpage for future studies.
vi. A combination of factors is considered to find the optimal solution to minimize the warpage of diameter. The fit value is 0.09 mm which is considerably lower than the experimental warpage value. The combination of factors that optimize the response is temperature gradient 0.28 (°C/mm), 0.3 mm (high level, 2) layer thickness, 50 mm/sec (low level, 1) print speed, and 20 % (low level, 1).

FUTURE ENHANCEMENT

The following considerations can be made for further work in this field.

i. The accuracy of the regression models can be increased by performing a higher number of replicate runs in the experiments.
ii. Interlayer waiting time and other continuous factors related to the FDM process can be included in combination with temperature gradient to achieve a predictive model with a higher R-squared R square value which will give a better fit to the experimental data.
iii. The aim of this experimental study is to understand the defects which occur in simple solid geometries. The effects of thermal deviations for complex shapes can be explored in future research studies.
iv. PLA material is utilized for printing the components in this experiment. Ensuing studies on FDM can focus on the variation in finished quality of components when ABS and other such material is used.
v. Subsequent studies can aim at experimentation in a controlled environment with a closed chamber instead of ambient conditions like those of the current study. The difference in responses will help gain a better understanding of shrinkage and warpage phenomenon.
vi. It is suggested that the study be extended further in future to explore the effects of thermal deviations for complex shapes.

ACKNOWLEDGEMENT

The authors acknowledge the RPT Lab, Department of Mechanical Engineering at SRM Institute of Science and Technology for providing the facility and kind co-operation to handling the experiments as successful.

REFERENCES

[1] A.K. Sood, R.K. Ohdar, and S.S. Mahapatra,. “Parametric appraisal of fused deposition modelling process using the grey Taguchi method”, *Proceedings of Institute of Mech. Engg. Part-B:Journal of Engineering Manufacture*, vol.224, no. 1, pp.135-145, 2009.
[2] A.Armillotta, M. Bellotti, and M. Cavallaro, “Warpage of FDM parts: Experimental tests and analytic model”, *Robotics And Computer Integrated Manufacturing*, vol. 50, pp. 140-152, 2018.
[3] D.Croccolo, M. De Agostinis, G. Olmi, “Experimental characterization and analytical modelling of the mechanical behaviour of fused deposition processed parts made of ABS-M30”, *Computational Material Science*, vol. 79, pp.506-518, 2013.
[4] H. Prajapati, D. Ravoori, and A. Jain, “Measurement and modeling of filament temperature distribution in the standoff gap between nozzle and bed in polymer-based additive manufacturing”, *Additive Manufacturing*, vol. 24, pp.224-231, 2018.
[5] E. Malekipour, S. Attoye, and H. El-Mounayri, “Investigation of layer based thermal behavior in fused deposition modeling process by infrared thermography”, *Procedia Manufacturing*, vol. 26, pp.1014-1022, 2018.
[6] N.G. Morales, T.J. Fleck, J.F. Rhoads, “The effect of interlayer cooling on the mechanical properties of components printed via fused deposition”, *Additive Manufacturing*,vol. 24, pp.243–248, 2018.
[7] O.A. Mohamed, “Optimization of fused deposition modeling process parameters: A review of current research and future prospects”, *Advances in Manufacturing*, vol. 3, no. 1, pp.42-52, 2015.

[8] S.J. Raykar, and D.M. D'Addona, "Selection of best printing parameters of fused deposition modeling using VIKOR," *Materials Today Proceedings*, vol. 27, pp. 344-347, 2020.
[9] T.J. Coogan, and D.O. Kazmer, "Inline rheological monitoring of fused deposition modeling", *Journal of Rheology*, vol. 63, pp. 141-155, 2019.
[10] Y. Tlegenov, W.F. Lu, and G.S. Hong, "A dynamic model for current-based nozzle condition monitoring in fused deposition modelling". *Progress in Additive Manufacturing*, vol. 4, pp. 211-223, 2019.
[11] O.A. Mohamed, S.H. Masood, and J. Bhowmik, "Optimization of fused deposition modeling process parameters for dimensional accuracy using I-optimality criterion," *Measurement*, vol.81, pp.174-196, 2016.
[12] A. Dey, D. Hoffman, and N. Yodo, "Optimizing multiple process parameters in fused deposition modeling with particle swarm optimization," International Journal of Interactive Design and Manufacturing, vol. 14, pp. 393–405, 2020.
[13] M. Kamaal, M. Anas, H. Rastogi, N. Bhardwaj, and A. Rahaman, "Effect of FDM process parameters on mechanical properties of 3D-printed carbon fibre–PLA composite", *Progress in Additive Manufacturing*, vol.6, pp.63-69, 2021.
[14] O.S.N. Raj, and S. Prabhu, "Analysis of multi objective optimization using TOPSIS method in EDM process with CNT infused copper electrode," *International Journal of Machining and Machinability of Materials*, vol. 19, no. 1, pp. 76-94, 2017.
[15] R. Ambigai, and S. Prabhu, "Fuzzy logic algorithm based optimization of the tribological behavior of Al-Gr-Si3N4 hybrid composite," *Measurement*,vol. 146, pp.736-748, 2019.
[16] R. Ambigai, and S. Prabhu, "Fuzzy logic algorithm-based optimization of heat transfer and thermal conductivity behaviour of Al–Si3N4 Nano and Al–Gr–Si3N4 hybrid composite," *Journal of Thermal Analysis and Calorimetry*, vol.147, pp.4059-4071, 2022.
[17] D.S.Stephen, and P. Sethuramalingam, "Optimization of grinding titanium with 2%CNT-CBN wheel using TOPSIS," *Materials and Manufacturing Processes*, Online first, 16th Feb.2022.
[18] M. Müller, P. Jirk, V. Šleger, R.K. Mishra, M. Hromasová, and J. Novotný, "Effect of infill density in FDM 3D printing on low-cycle stress of bamboo-filled PLA-based material," *Polymers,* vol. 14, p. 4930, 2022.